

T. Mulder · M. Voisset · P. Lecroart · E. Le Drezen
E. Gonthier · V. Hanquiez · J.-C. Faugères
E. Habgood · F. J. Hernandez-Molina · F. Estrada
E. Llave-Barranco · D. Poirier · C. Gorini · Y. Fuchey
A. Voelker · P. Freitas · F. Lobo Sanchez
L. M. Fernandez · N. H. Kenyon · J. Morel

The Gulf of Cadiz: an unstable giant contouritic levee

Received: 25 March 2002 / Accepted: 20 January 2003 / Published online: 15 March 2003
© Springer-Verlag 2003

Abstract Recent multibeam bathymetry and acoustic imagery data provide a new understanding of the sedimentary system located in the Gulf of Cadiz which is under the influence of a strong current, the Mediterranean Outflow Water (MOW). When it comes out from the Strait of Gibraltar, the MOW is either channelled along major or secondary channels, or spills over a sedimentary levee. Frequent earthquakes and the constant current shearing generate widespread sediment deformation and instability of contourite deposits. Secondary channels can form by retrogression following an initial failure. At their mouth, sediment accumulates in the form of small sandy contourite lobes. These observations suggest that the Gulf of Cadiz system shares many similarities with channel–levee complexes formed by turbidity current activity. The main difference is that,

in the Gulf of Cadiz, the main process is a strongly flowing saline current which locally interacts with gravity processes.

Introduction

The Gulf of Cadiz is located in the eastern Atlantic Ocean, northwest of the Strait of Gibraltar, along the Spanish and Portuguese continental margins (Fig. 1). The study area is located at the termination of the Azores–Gibraltar transform fault (Srisvastava et al. 1990) where Iberia and Africa converge in a NNW–SSE direction (Argus et al. 1989).

T. Mulder (✉) · P. Lecroart · E. Gonthier · V. Hanquiez
J.-C. Faugères · D. Poirier · J. Morel
Département de Géologie et Océanographie,
UMR 5805 EPOC, Université Bordeaux 1,
Avenue des Facultés,
33405 Talence cedex, France
E-mail: t.mulder@epoc.u-bordeaux.fr

M. Voisset · E. Le Drezen
IFREMER, DRO/GM, Centre de Brest,
B.P. 70, 29280 Plouzané, France

E. Habgood · N. H. Kenyon
Challenger Division for Seafloor Processes,
Southampton Oceanography Centre,
Empress Dock, Southampton SO14 3ZH, UK

F. J. Hernandez-Molina
Dpto. de Geociencias Marinas,
Facultad de Ciencias,
36200 Vigo (Pontevedra), Spain

F. Estrada
CSIC, Instituto de Ciencias del mar,
Paseo Juan de Borbon s/n,
08039 Barcelona, Spain

E. Llave-Barranco
Servicio de Geología Marina, Instituto Geológico y Minero,
C/Rios Rosas 23, 28003 Madrid, Spain

C. Gorini
Bâtiment SN5, Université Lille 1,
59655 Villeneuve d'Ascq cedex, France

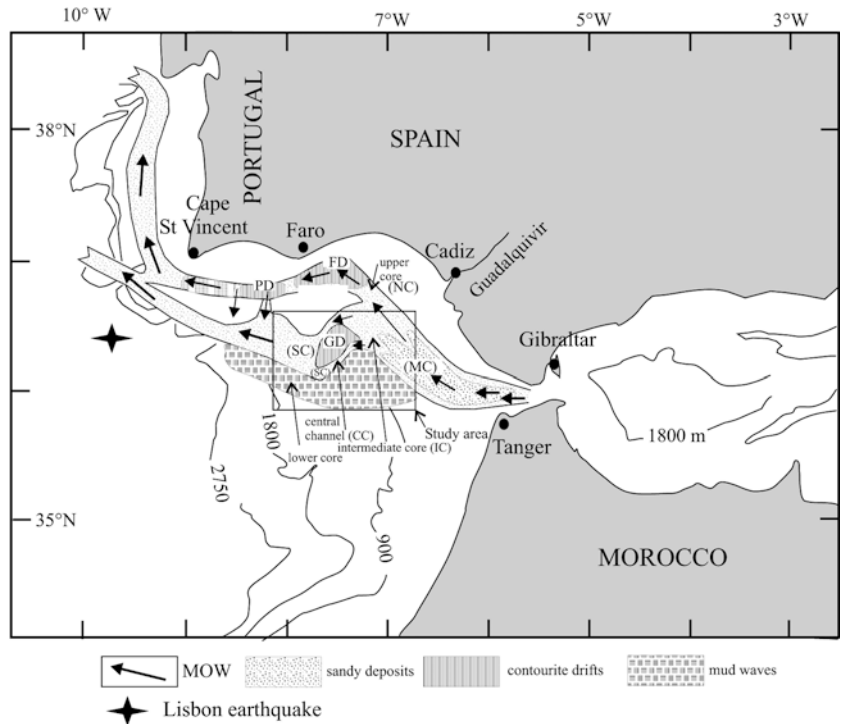
Y. Fuchey
Département de Géologie, Université de Genève,
13 rue des maraîchers, 1211 Genève, Switzerland

A. Voelker · P. Freitas
Departamento de Geologia Marinha,
Instituto geologico e Mineiro,
Estrada de Portela, Zambujal,
2720 Alfragide, Portugal

F. L. Sanchez
CIACOMAR, Universidade do Algarve,
Avenidas Forças Armadas s/n.,
8700 Olhao, Portugal

L. M. Fernandez
Instituto Espanol de Oceanografia,
c/o Corazon de Maria 8, 5 planta,
28002 Madrid, Spain

Fig. 1 General map of the Gulf of Cadiz showing the three cores of the Mediterranean Outflow Water. *Bold arrows* indicate MOW direction. *CC* Central channel; *GD* Guadalquivir Drift; *FD* Faro Drift; *IC* intermediate core of the MOW; *MC* main MOW channel; *NC* northern channel of the MOW; *PD* Portimão Drift; *SC* southern channel of the MOW



The present sedimentation in the Gulf of Cadiz is controlled by the Mediterranean Outflow Water (MOW), a strong current which has been active since the Pliocene, after the Mediterranean basin was flooded after the Messinian salinity crisis (Mougenot and Vanney 1982). This activity is attested by the construction of large contourite drifts such as the Faro (Faugères et al. 1984, 1985a; Stow et al. 1986; FD in Fig. 1), the Portimão (PD in Fig. 1), and the Guadalquivir drifts (Somoza et al. 1997; GD in Fig. 1). These are generally plastered over salt diapirs (Malod 1982) or tectonic highs such as the Guadalquivir Bank. Cores taken in the top part of the drifts show thick accumulations of thoroughly bioturbated, fine-grained sedimentary sequences with typical thicknesses of 0.2–1.2 m (Gonthier et al. 1984). The construction of the drifts is cyclic, being controlled by climatic and eustatic oscillations. Eustasy either widens or restricts the pathway between the Mediterranean and the Atlantic during relative highstands and lowstands, respectively (Faugères et al. 1985b; Grousset et al. 1988; Vergnaud-Grazzini et al. 1989), thereby modifying both the flow path and the current intensity of the MOW. Presently, the MOW is a strong, warm (13 °C), and saline (38 g l⁻¹) current which flows out of the Mediterranean below the Atlantic waters (Ambar et al. 1976; Ambar 1983). It reaches core velocities of > 2.5 m s⁻¹ along the continental slope near Gibraltar and still flows at 0.2 m s⁻¹ off Cape St. Vincent in Portugal (Meincke et al. 1975; Johnson et al. 2002). A current named the Atlantic inflow (Nelson et al. 1999) flows back from the Atlantic into the Mediterranean. When reaching the gulf, the MOW is rapidly deflected towards the north due to the Coriolis force. West of

06°20'W, it splits into two cores which flow along the seabed at water depths of 300 to 1,500 m (Fig. 1). The upper core is a geostrophic current which follows a northerly path, bending westwards along the Spanish and Portuguese continental slopes at depths of 300–600 m. The lower core is an ageostrophic current which flows directly westwards from the Strait of Gibraltar. It divides into an intermediate core flowing between 600- and 900-m water depths, and a deep core flowing between 900 and 1,500 m (Madelain 1970). At approximately 1,300–1,500 m water depths in the western part of the Gulf of Cadiz, the MOW is disconnected from the seafloor and becomes a water mass intercalated between the deep and intermediate Atlantic waters. The velocity of the MOW is strongly influenced by seafloor morphology (Heezen and Johnson 1969; Madelain 1970; Mélières 1974). Thorpe (1972, 1976), for example, reported an average local current speed of 0.4 m s⁻¹ which increases to 0.8–1 m s⁻¹ when the flow is channelized. On a plateau such as the Faro drift, the MOW spreads out and its velocity can decrease from 0.3–0.4 to 0.1–0.2 m s⁻¹. On contourite drifts, where its velocity decreases, sedimentation rates vary from 5 to 13 cm 1,000 year⁻¹ on the upper and middle slopes, respectively (Nelson et al. 1993). An extreme value of 38 cm 1,000 year⁻¹ has been reported by Schönfeld and Zahn (2000).

The sediments carried by the MOW are derived from Spanish rivers, particularly the Guadalquivir River. Initially, these are either transported rapidly towards Gibraltar by along-shelf currents or they are temporarily trapped on the shelf before being reworked by gravity processes. Finally, when arriving on the Gibraltar slope,

the particles are entrained by the energetic MOW. The average grain size of the surface sediments decreases when the MOW velocity decreases. Following the MOW from Gibraltar, one at first encounters gravel lags followed by sand patches as well as sand and silt waves (Habgood et al., personal communication), mixed silt and mud waves, and finally mud waves (Kenyon and Belderson 1973; Gardner and Kidd 1983; Nelson et al. 1993, 1999). All these studies present the global water circulation and give a general view of the sediment distribution in the Gulf of Cadiz. Tectonic studies focused on deep structures are in general disconnected from surface observation.

In this paper, we present a new morphology for the Gulf of Cadiz, derived from multibeam bathymetry and acoustic imagery, with an accuracy which has to date never been achieved in this area. These data are used to explain how tectonics can force flow dynamics and sediment distribution in the gulf. This paper also shows how surface sedimentary structures are related to deep deformation or to tectonic activity.

Material and methods

The data presented in this paper were collected during the CADISAR cruise on the RV “Le Suroît” in August 2001. Bathymetric data and acoustic imagery were acquired with a SIMRAD EM300 multibeam echosounder. This system operates at a frequency of 30 kHz and

a maximum angle of 150°, the swath width varying between 300 and 5,000 m at water depths of 10 and 5,000 m, respectively. It was operated at a speed of 5–5.5 knots. The acoustic data were corrected for salinity and density effects using 5 CTDs (SBE19 probes) and 35 thermoprobes (Sippican). The top of 25 Kullenberg piston cores was used to control the grain size and interpret the acoustic imagery.

Results

The area mapped during the CADISAR cruise is located south of the northernmost MOW channel (Fig. 1). It covers the area located between 35°40'N and 36°30'N, 06°30'W and 08°10'W (Figs. 2 and 3). The bathymetry ranges from 600 m in the NE corner of the study area to 1,920 m in the southwestern corner. The average regional slope remains less than 1° towards the SW.

Six features can be distinguished in the study area. Four are channels draining the MOW cores: (1) the main MOW channel close to the Strait of Gibraltar (MC in Fig. 1) which drains the three superposed cores, (2) the northern MOW channel (NC in Fig. 1) which drains the upper core, (3) the central MOW channel (CC in Fig. 1), and (4) the southern MOW channel (SC in Fig. 1). Both central and southern channels drain the lower core. Two are inter-channel areas: (5) the area between the central and southern channels, and (6) the area south of the southern channel and west of the main

Fig. 2 High-resolution (30×30-m grid) EM300 bathymetric map of the part of the Gulf of Cadiz studied during the Cadisar cruise. *Black numbers* refer to Fig. 4

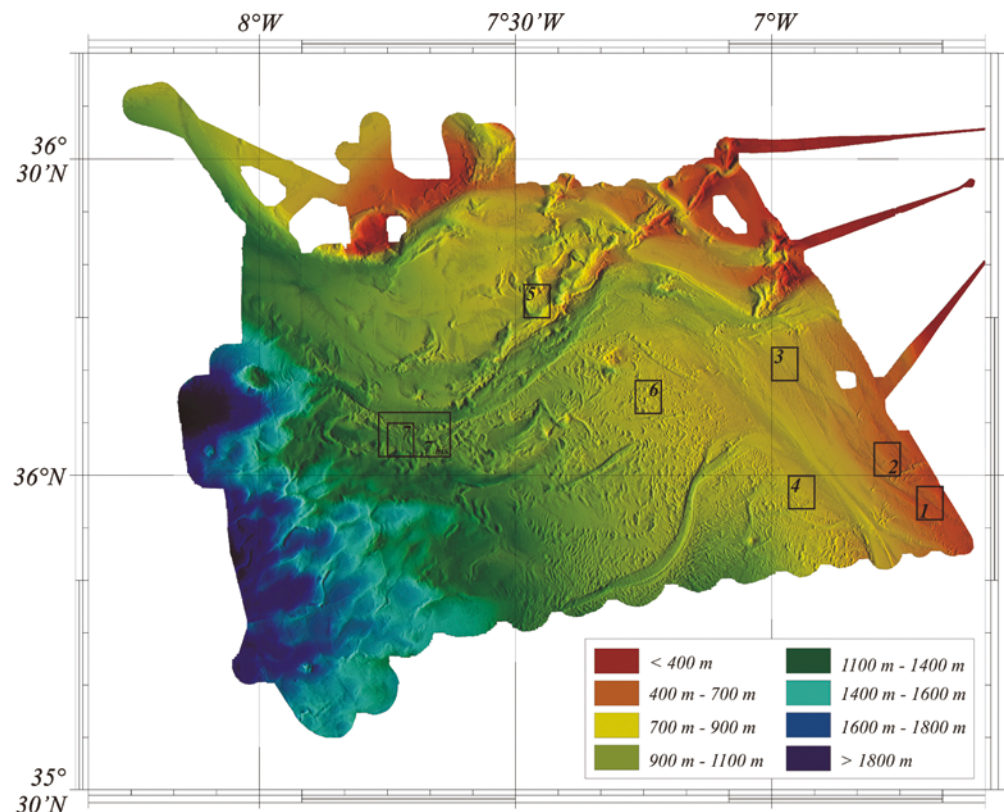
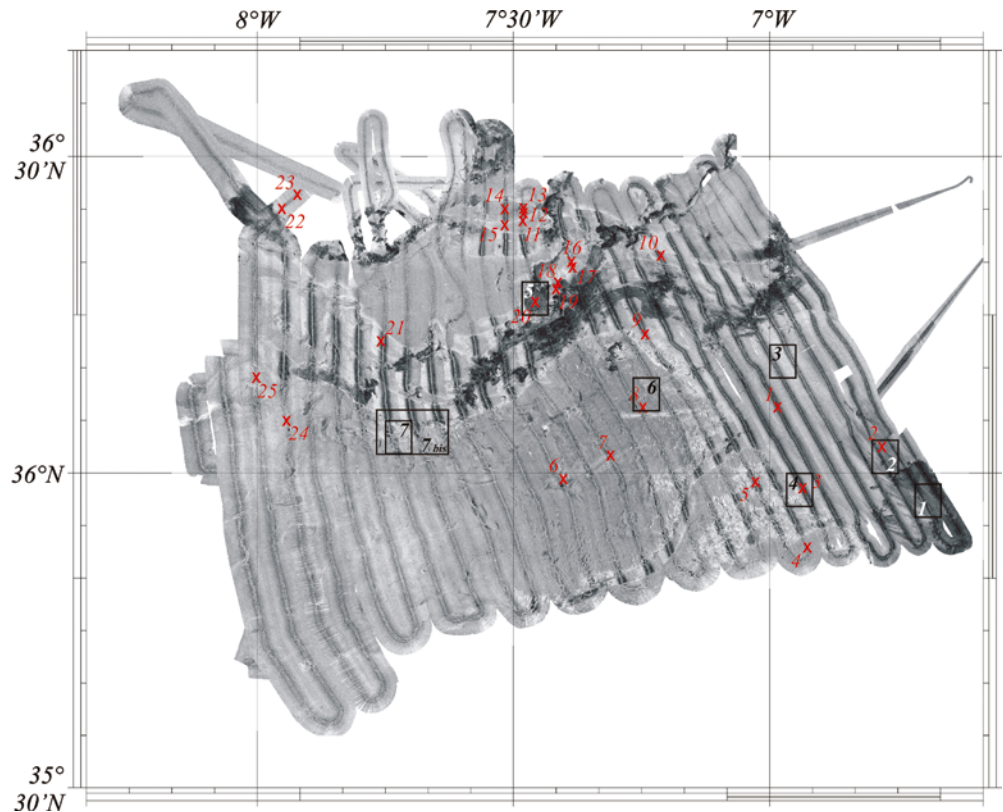


Fig. 3 High-resolution (12.5×12.5-m grid) EM300 acoustic imagery map of the part of the Gulf of Cadiz studied during the Cadisar cruise. *Black numbers* refer to Fig. 4. *Red numbers* are core locations



channel. Channels have a “striped” backscatter, indicating high reflectivity (Fig. 3). The stripes appear because backscatter of beams reflecting vertically to the ship are stronger than the backscatter of beams reflecting at lower angles. This high backscatter indicates that the channels are dominated by erosional processes and/or they are made of coarse-grained consolidated sediments.

The main MOW channel

The main MOW channel (MC in figures) appears in the southeast corner of the study area (Figs. 2, 3 and 5) where it extends out from the Strait of Gibraltar. It drains the three parallel flowing MOW cores. On the maps of Figs. 2 and 3, where only its western and deepest part is visible, it is more than 16 km wide. The channel is NNW aligned, its floor dipping towards the west, i.e. following the same trend as the dip of the regional slope. The decrease in flow strength of the MOW away from the Strait of Gibraltar is particularly evident on this channel floor. In the southeastern corner of the acoustic map, east of 06°45'W and south of 36°01'N, the channel shows high backscatter (Fig. 3) with giant furrows (length: 1–6 km; width: 100–250 m) and scours (1 in Fig. 4 and GF in Fig. 5), which are aligned at 105° close to Gibraltar, progressively bending towards 140°. On tidal shelves, furrows form beneath currents stronger than 1 m s^{-1} (Belderson et al.

1982). This suggests that these features are the result of erosion by the high MOW velocity (Kenyon and Belderson 1973; Nelson et al. 1999). The high reflectivity is related to the presence of gravels on the channel floor (Kenyon and Belderson 1973; Nelson et al. 1999; Fig. 3). The deposits of this area are interpreted to represent a gravel lag, i.e. a deposit in which all the particles finer than coarse sand have been winnowed by strong currents.

The channel then bends towards the north (south bend, SB in Fig. 5). The classical shape of the meander suggests a southerly or southwesterly migration of this bend. Between 36°01'N and 36°08'N, and east of 6°58'W, giant furrows are still present. They are associated with ribbons (length: 3–9 km; width: 125–1 km) of the type described by Kenyon (1970; 2 in Fig. 4), and the backscatter is of lower intensity on the reflectivity map (Fig. 3). Erosion still dominates, but particles are probably finer than further south, suggesting the presence of coarse sand lag deposits. The northern and the western parts of the main channel are areas in which the MOW velocity apparently does not exceed 1.5 m s^{-1} (Meinke et al. 1975; Johnson et al. 2002). These areas are covered only with coarse-grained sediment waves (3 in Fig. 4 and SW in Fig. 5), mainly sand waves, their crests being oriented 40°N which indicates a NW trend on average (130°) of the MOW flow direction. Such waves are frequently associated with geostrophic currents (Damuth 1975), deep-sea turbidite activity (Migeon et al. 2000, 2001; Gervais et al. 2001),

or the interaction of both current types (Viana 1998; Viana et al. 1998; Faugères et al. 1999). At the western side of the channel, wave crests have a north-north-easterly orientation (15°), indicating that part of the MOW also flows westwards. In the divergence area ($36^\circ18'N$, $07^\circ02'W$, DA1 in Fig. 5), the main channel forks into a northern and a southern channel.

The northern channel

The northern channel is just visible in the northeastern corner of the map. It is 12 km wide, more than 120 m deep, and drains the upper core flow of the MOW. Just north of the divergence area, the northern channel crosses a NE–SW-oriented submarine valley (SV1 in Fig. 5) ($36^\circ22'N$, $07^\circ02'W$). This valley forms a connection between the upper and the lower cores of the MOW. In this valley, particle-laden gravity flows can interact with the MOW. A similar valley (SV2) oriented at 52° appears in the northeastern corner of the map ($36^\circ25'N$, $07^\circ13'N$). The northern and the southern channels are separated by a 120-m-high escarpment dipping towards the SW and striking in a NW–SE trend. It extends between $36^\circ19'N$, $07^\circ02'W$ and $36^\circ22'N$, $07^\circ16'W$. This escarpment could indicate either a tectonic control or an evolution in MOW dynamics. In this latter case, this would suggest that the northern channel either formed before the southern channel or that the southern core drained by the southern channel is presently more energetic than the northern core which occupies the northern channel.

The southern channel

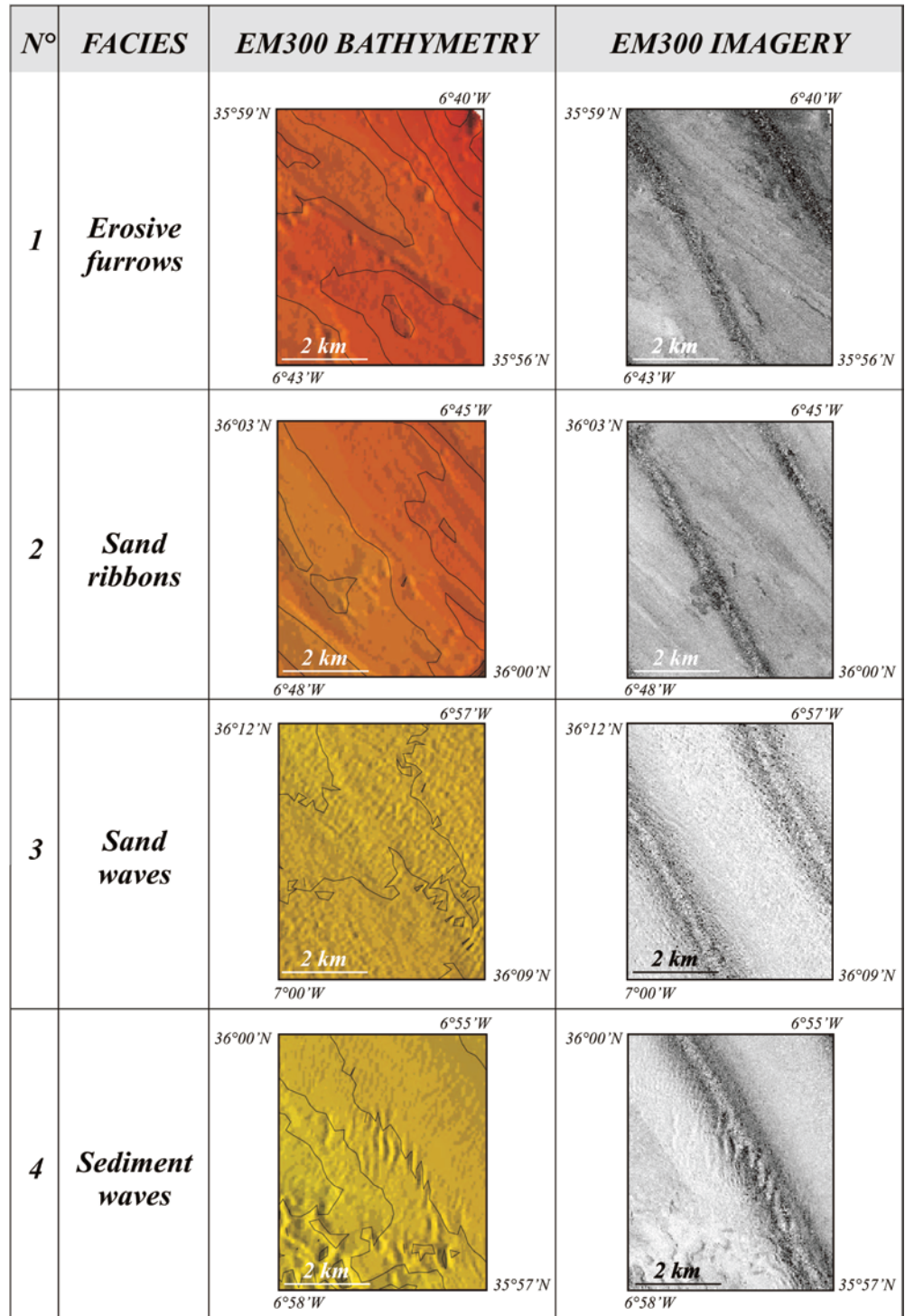
The southern channel corresponds to channel 2 of Kenyon and Belderson (1973; Figs. 2, 3 and 5) which drains the lower core of the MOW. It is more than 300 m deep in its eastern part, more than 150 m deep in its western part, and 4 to 10 km wide. West of the divergence area, it bends towards the SW (northern bend, NB in Fig. 5). This bend shows a classical erosional bank in the north, underlain by the escarpment separating it from the northern channel (Fig. 2), and a depositional embankment in the south. High sedimentation rates on this side are indicated by the widespread sediment deformation and flow towards the SSW, and are consistent with high backscatter on the reflectivity map (Fig. 3). The northern bend thus evidently migrates northwards. The southern channel follows a lineament oriented at 60° (DL in Fig. 5). This lineament extends from $36^\circ07'N$, $07^\circ36'W$ to $36^\circ23'N$, $07^\circ18'W$ and consists of a series of topographic highs and lows reaching 350–400 m. Some are circular and are hence interpreted to represent diapirs of Triassic evaporites (Mougenot 1988; 5 in Fig. 4). Others have a more linear trend and are interpreted as submarine scarps of

outcropping rocks or very consolidated sediments. Most of the topographic lows also have circular shapes with an outer rim and a central closed depression (e.g. at $36^\circ16'N$, $07^\circ28'W$ or $36^\circ18'N$, $07^\circ24'W$). They are interpreted as collapse structures due to dissolution of Triassic evaporites. The northernmost valley crossing the northern channel (SV2 in Fig. 5) is a continuation of this lineament. At the western extremity of the map, and just west of the western bend, the southern channel forks into two branches. The larger of the two extends northwards and constitutes the continuation of the southern channel. The smaller and narrower one forms a secondary channel (SeC in Fig. 5) which continues south of a topographic high (TH2 at $36^\circ09'N$, $08'W$) and terminates in a small elongated deposit having a backscatter intensity which is slightly lower than the surrounding areas. It is interpreted to represent a depositional lobe (Lo1 in Fig. 5 at $36^\circ05'N$, $08^\circ08'W$) analogous to sedimentary bodies located in deep-sea turbiditic environments (Normark 1970).

The central channel

The central channel drains the intermediate MOW core (Figs. 2, 3 and 5). It is 150 m deep in its eastern part and more than 300 m deep in its western part, its width varying between 4 and 6.5 km. It diverges from the northern channel at $36^\circ22'N$, $07^\circ17'W$ (DA2 in Fig. 5). Just west of the divergence area, the channel forks (F in Fig. 5)/(TH in Fig. 5) rather suddenly due to a topographic high to form a northern and a southern branch (Nbr and Sbr in Fig. 5, respectively). The high backscatter of the obstacle suggests that it is a rock outcrop of similar nature as the lineament which follows the southern channel (Fig. 3). Just west of the obstacle, the floor of both branches shows high backscatter which rapidly decreases downslope (Fig. 3). This correlates with the bathymetry (Fig. 2). Just past the obstacle, the depth of the two branches at first increases rapidly, followed by a just as rapid decrease westwards. This suggests that the velocity of the intermediate MOW core increases strongly due to channelling. However, the energy of the flows in the two branches rapidly dissipates downvalley due to spreading, preventing substantial erosion westwards. The area between the two branches, i.e. westward of the topographic high, is characterized by a very low backscatter. This plateau rises 80–90 m above the channel floors. It is interpreted to represent an “energy shadow zone” (ZES in Fig. 5), i.e. a low-energy area where fine-grained deposition predominates due to the loss of velocity and competency of the MOW behind the topographic obstacle. This explains the very smooth bathymetry at this location (Fig. 2). Just north of this area, meandering channels are visible (MeC in Fig. 5), indicating the activity of particle-laden gravity flows which could interact locally with the MOW. Towards the west, the two branches converge to again form a

Fig. 4 Examples of EM300 bathymetry and imagery for erosive furrows (1), sand ribbons (2), sand waves (3), sediment waves (4), diapirs (5), pockmarks (6) and sediment instabilities in areas of intense deformation (7 and 7bis). Location in Figs. 2 and 3



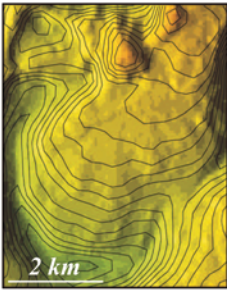
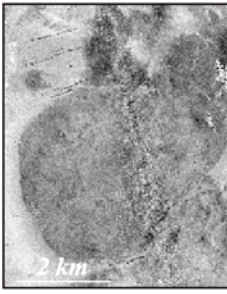
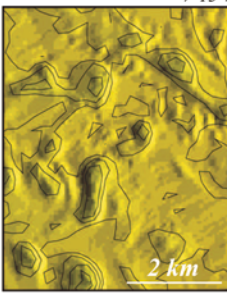
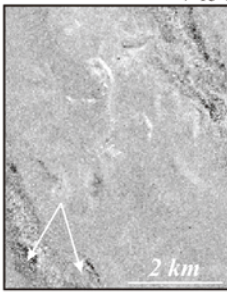
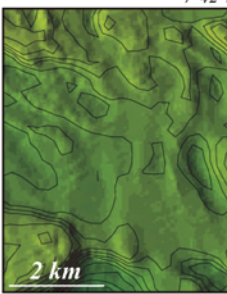
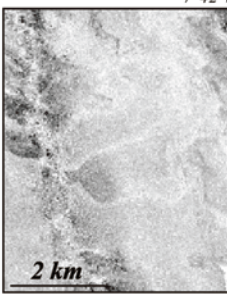
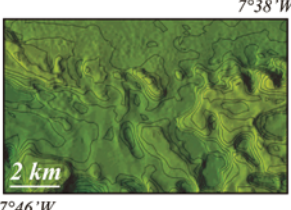
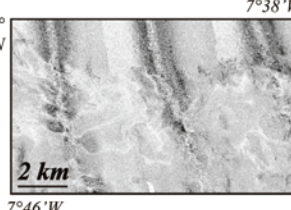
single channel which is bordered in the northwest by the Guadalquivir drift (GD in Fig. 5).

Area between the central and southern MOW channels

The area located between the central and southern MOW channels (Figs. 2, 3 and 5) has the same acoustic facies as

the zone of energetic shadow described above for the central channel. This area is flat and situated 200 m above the floor of the southern MOW channel (Fig. 2). It is protected against MOW flow energy by the 60° lineament which follows the southern MOW channel. It is also interpreted as a low-energy area (LEA) reached only by fine-grained particles. This explains the very smooth bathymetry and the low-acoustic backscatter (Fig. 3).

Fig. 4 (Contd.)

N°	FACIES	EM300 BATHYMETRY	EM300 IMAGERY
5	<i>Diapir</i>		
6	<i>Pockmarks</i>		
7	<i>Instability</i>		
7 bis	<i>Instability</i>		

Area south of the southern MOW channel

The area located south of the southern MOW channel and west of the main MOW channel (Figs. 2, 3 and 5) has an average dip of 0.48° to the west. In the eastern part (between 07°00'W and 07°26'W), at water depths ranging between 800 and 1,150 m, the average slope is 0.42°. In the western part, between 1,150 and 1,800 m

(west of 7°26'W), the slope is 0.57°. The eastern part is located 70–80 m above the floor of the main channel. The top of this topographic high, called “longitudinal sandy ridge” by Kenyon and Belderson (1973), shows sediment waves with their crests oriented at 150°–180°, indicating a 255° flow direction of the MOW (4 in Fig. 4). In this area, we observe two disturbed zones characterized by low backscatter (AID in Fig. 5; 7 and

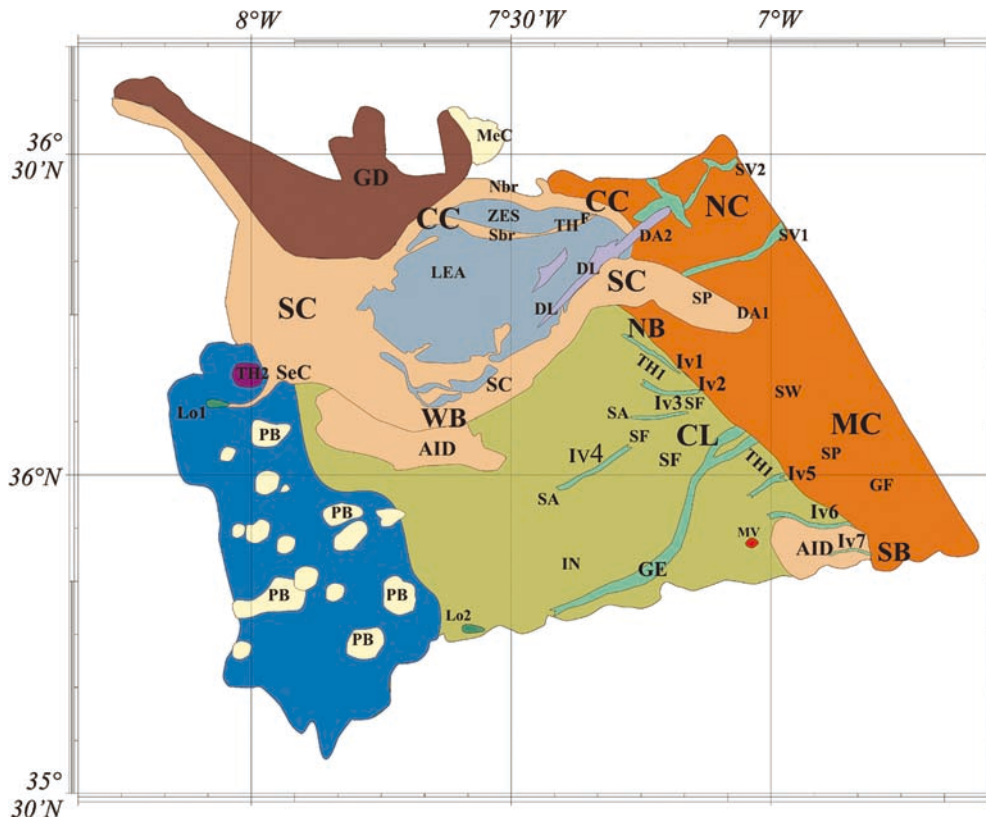


Fig. 5 Interpretation of the EM300 bathymetry and acoustic facies produced using Caribes software from Ifremer. *AID* Area of intense sediment deformation; *CL* contouritic levee; *DA1* divergence area between northern and southern channels; *DA2* divergence area between northern, and central channels; *DL* lineaments of diapirs and rock outcrops; *CC* central channel; *F* fork of central channel; *GD* Guadalquivir Drift; *LEA* area with low-energy sedimentation between central and southern MOW channels; *GE* Gil Eanes channel; *GF* giant furrows and scours; *IN* interconnected network of sediment wave crests; *Iv* (1, 2, 3, 4, 5, 6 and 7) inactive channels; *Lo* (1 and 2) lobe; *MC* main MOW channel; *MeC* meandering channels; *MV* mud volcano; *NB* north bend; *Nbr*: northern branch of the central channel; *NC* northern channel of the MOW; *SF* sediment failure; *PB* ponded basins (ancient sediment failures); *SA* sediment accumulation; *SB* Southern bend; *Sbr* southern branch of the central channel; *SC* southern channel; *SeC* secondary channel; *SF* slope failure; *SP* sand patches; *SV1*, *SV2* submarine valleys; *SW* sediment waves; *TH* topographic high; *WB* Western bend; *ZES* Zone of energetic shadow. *Orange* NC and MC; *beige* SC and CC; *green* CL; *brown* GD; *green* GE, Sv and Iv; *grayish green* ZES and LEA; *deep green* Lo; *pink* TH2; *red* MV; *yellow* MeC

7bis in Fig. 4). They are located just west of the southern bend (SB in Fig. 5), and south of the western bend (WB in Fig. 5), the top of the topographic high (TH1 in Fig. 5) also being affected by local sediment instabilities. Large-scale shallow slope failures (SF in Fig. 5) and flows are visible. Their shapes vary from circular, indicating sediment collapse without transport, to elongate or bottlenecked (Prior and Coleman 1979), indicating sediment flow. The deformation structures have morphologies which mimic sediment waves (Faugères et al. 2002), and the distinction between the two may some-

times be confusing. The very low backscatter, the absence of a clear trend in observed “wave” direction (east of the western bend), and the lack of continuity in “wavelength” strongly suggest that sediment deformation dominates in this region.

The eastern part of the area located south of the southern MOW channel is also characterized by the presence of secondary submarine channels (Habgood et al., personal communication). These channels share a number of morphological features. Most of the channels are oriented downslope, i.e. westwards. Their average direction is N235° with extreme values ranging between 195° and N275° (except IV1 in Fig. 5, direction 315°), which is consistent with the direction of the lineament bordering the southern channel. Their upper part shows a concentration of circular failure scars. Topographic highs are visible at their western (downslope) extremities (SA in Fig. 5). One of these channels, the Gil Eanes channel (GE in Fig. 5; Kenyon and Belderson 1973) which drains the deep core of the MOW, is active and connected upslope to the main MOW channel. CTD measurements confirmed the presence of MOW flowing along the channel floor. This channel is more than 40 km long and 2.5 km wide at its connection with the main MOW channel, from where it rapidly narrows to 1–1.8 km. It is more than 100 m deep and has a typical U-shape in cross section, with very steep sidewalls all along its path. The north side of the channel is bordered by a low backscatter area forming a fringe over 1 km wide (Fig. 3) and of low relief (Fig. 2). This fringe has a similar acoustic texture as the area of intense

deformation. The channel is floored with sediment waves, probably composed of sand as indicated by the high backscatter intensity. It ends at 1,200-m water depth where two areas are developed which have an acoustic backscatter slightly lower than the surrounding areas (35°45'N, 07°37'W). These are interpreted to represent small depositional lobes (Lo2 in Fig. 5; Habgood et al., personal communication).

Northwest of the Gil Eanes channel, four other channels occur which are currently disconnected from the main MOW channel (Iv1, Iv2, Iv3 and Iv4 in Fig. 5) and, for this reason, interpreted as inactive channels. They are less than 0.8 km wide, between 13 and 17 km long, and do not show high backscatter of their floor. Conversely, channels south of Gil Eanes have a high backscatter, similarly to that of Gil Eanes. They are 11 to 19 km long and 1 to 1.5 km wide. Two of these run a few kilometres parallel and south of Gil Eanes at 35°56.5'N, 07°W and 35°59'N, 07°W (IV5 and IV6 in Fig. 5). They may still be connected to the main MOW channel. The last channel is located at the southeastern extremity of the map (IV7 in Fig. 5). It is still connected to the main MOW channel and may be presently active. Just north of Gil Eanes, an area centred around 35°43'N, 07°22'W is covered with a network of fine-grained, interconnected sediment waves (Gervais et al. 2000). The directions of wave crests range between 30° and 155°, suggesting complex flow hydrodynamics and possible flow interactions. The westernmost part of the area located south of the southern MOW channel shows circular to egg-shaped depressions (PB in Fig. 5). Each of these is bordered by a 100–200 m high escarpment in the east and by a small topographic high in the west. They are interpreted to indicate large sediment failures heading westwards. The eastern escarpment and the western mounds would then represent failure scars and sediment accumulations, respectively. They probably form small ponded basins. In the southeasternmost part of the map, the St. Petersburg mud volcano (Kenyon et al. 2000; MV in Fig. 5) is visible at 35°54'N, 07°02'W, indicating upward motion of deep fluid.

Discussion

The Gulf of Cadiz: a giant contouritic levee?

The area extending south of the southern MOW channel and west of the main MOW channel shows evidence of sediment accumulation. For a start, it represents a topographic high when compared to the main channel. This topographic high has fields of sediment waves superimposed on its eastern and middle parts (the interconnected network). This suggests that the flow strength and sediment load are sufficiently high to construct large sedimentary bedforms. In addition, the crest orientation of the sediment waves in the western part of the main channel, and in the eastern part of the area located west of this main channel suggests westward flow of the

MOW at this location. The waves located close to the main channel have linear crests, indicating formation by unidirectional currents. The interconnection of wave crests to the west suggests that flow directions tend to become more complex downslope. Part of the MOW flows westwards, above the topographic high bordering the western part of the main channel. The high sedimentation rates indicative of sediment deposition by loss of flow competence is also underlined by the widespread occurrence of sediment failures. The scars (SF in Fig. 5) show that the failures involve only the uppermost part of the deposits. Freshly deposited sediments, which still have a high water content, are easily remobilized despite the small slope. The channel floor, by contrast, is covered by erosive structures and coarse sediments, indicating high MOW flow velocities. The topographic high bordering the main channel is also covered by sediment waves, indicating deposition and a westward-decreasing flow velocity. This suggests that part of the flow extends over the levee where it decelerates and hence deposits its sediment load. Evidence for spill-over is emphasized by the local occurrence of intense deformation. Such areas are located just past the eastern and western bends. There, as indicated by sediment waves, the flow direction is approximately 45° from the direction of the channelled flow before the southern bend. The location of sediment waves and the orientation of their crests are analogous to those found on levees situated after a meander of a submarine channel-levee complex in a deep turbidite system (Migeon 2000; Gervais et al. 2001). These turbiditic levees have recently been demonstrated to form by spill-over and flow stripping (Piper and Normark 1983; Peakall et al. 2000).

These observations suggest that the part of the Gulf of Cadiz located west of the main channel acts as a giant sedimentary levee, built by stacked contourites deposited by that part of the MOW which flows over the topographic high and, as a result, loses its competence. This structure differentiates from contourite drifts of McCave and Tucholke (1986) because one part of the flow remains channelled and flows parallel to the levee, whereas another part spills over and flows non-parallel to the levee. This association of spill-over and flow stripping is a very uncommon feature in contourite depositional systems. In the Gulf of Cadiz, this particularity is probably due to the existence of a high-velocity westerly flow due to the constriction imposed by the Strait of Gibraltar. The unusually high velocities reached by the MOW at the exit of the Strait of Gibraltar (1–3 m s⁻¹; Meincke et al. 1975; Johnson et al., 2002) are an order of magnitude higher than those usually associated with contour currents (0.1 m s⁻¹), being more in the range of velocities observed or calculated for turbidity currents (Migeon 2000). The constant shearing of sediment by the spilling MOW probably adds to the instability of the outer side of the levee.

The part of the MOW which does not spill over the levee is drained by the Gil Eanes channel. The channeling causes a strong flow acceleration, which explains

the steepness of its walls. This accelerated flow can then spill over the Gil Eanes channel wall and form a levee on the right-hand side of the channel, which would explain the topographic high and the intense deformation which appears along the northern but not on the southern channel margin. The spilling of fine particles only would explain the low backscatter. Finally, the Gil Eanes channel is a typical channel draining downwelling currents (Faugères et al. 1999). The depositional lobes observed at the end of secondary channels, and particularly at the end of Gil Eanes, can have three origins. (1) They can be due to flow expansion of the downwelling currents at the channel mouth. In this case, they would be contourite lobes composed of stacked contourite sequences. (2) They can be the mass-flow deposits related to the scars observed at the channel head. In this case, they would represent debris flow deposits (debrites). (3) The channelled gravity flows may have transformed into turbidity currents. In this case, the lobes may also have formed because of the loss of flow competence at the channel mouth. However, they would now represent turbiditic lobes composed of stacked turbidite beds.

Evidence for tectonic control of the MOW channels

The southern channel follows a tectonic lineament which is characterized by diapirs (Malod 1982). Also, the orientation of the Gil Eanes and the direction of the inactive channels in the area located south of the southern channel reflect the influence of the lineament. Mud volcanoes such as those observed in the Gulf of Cadiz (Gardner 2000; Gardner and Shashkin 2000) represent fluid escape structures which are frequently associated with tectonic activity, particularly in accretionary prisms such as for example the Barbados prism (Gribouard et al. 2001). In the Gulf of Cadiz, mud volcanoes are related to the presence of a deeply rooted body (olistostrom) with a slip surface at approximately 10 km below the seafloor (Lajat et al. 1975; Auzende et al. 1981; Maldonado et al. 1999). This structure is now interpreted as an accretion prism (Gutscher et al. 2002). These observations suggest that the structures observed in the study area are under tectonic control. The lineament could be the surface expression of a large, deep-rooted fault. The bathymetric change caused by the lineament locally exceeds 300 m. This fault-controlled structure has partially directed the MOW core, inducing it to split up. These subsurface features are consistent with the seismic activity observed in the Gulf of Cadiz and neighbouring areas, which is attested by the large ($M_w=8.5$) Lisbon earthquake (Zitellini et al. 1999) of 1755. This seismic activity could hence be responsible for some of the numerous sediment failures observed south of the southern channel. The ground acceleration induced by seismic waves can cause liquefaction of the sediment which can then begin to flow even at low slope gradients (Lewis 1971). If this mechanism applies, then

some of the circular structures could be interpreted as pockmarks produced by the upward movement of fluid from overpressurized deep layers in the wake of earthquake shocks (6 in Fig. 4).

Secondary channel formation

The secondary channels, in general, have directions which also follow the regional structural trends. However, the process of channel formation is still unclear. The slump scars in the head region may indicate that they are presently forming by retrogressive erosion. If correct, they would be young features and retrogression would be expected to continue until they merge with the main MOW channel. When merging, the newly connected channel would act in the same manner as the present Gil Eanes channel, and the topographic highs at the downslope extremity of the channel would represent mass-flow deposits. Conversely, sediment failures at the channel heads may be due to overloading and oversteepening, indicating rapid progradation. High sedimentation rates due to a loss of flow competence would induce frequent failures, particularly at the channel heads where slopes are locally steeper. Such progradation would end with a complete infilling of the channel. In this case, the secondary channels would be old features, and the topographic highs at the downslope end of the channels would be ancient lobes formed similarly to those observed at the distal end of the presently active Gil Eanes channel.

Important differences exist between the channels located north and south of Gil Eanes. Channels located north (Iv 1 to 4 in Fig. 5) have low backscatter, suggesting that they are presently filling with soft fine-grained sediments. Their heads are several kilometres away from the main MOW channel. Conversely, channels located south of Gil Eanes (Iv 5 to 7 in Fig. 5) have a high backscatter similar to that observed on the Gil Eanes channel floor, suggesting they are presently active and that their floors are affected by erosional processes caused by strong flow of the channelized MOW. These channels are either connected or have their heads very close to the main MOW channel. This would suggest that the channels located north of Gil Eanes are old channels which are progressively infilled, whereas the southern channels are young, actively developing features. This would also suggest that there is a north-south trend in channel formation, the age of the channels decreasing progressively towards the south. This can be explained by two mechanisms. The first is sedimentary. Because of the northward migration of the northern bend of the southern channel and the inferred southwest migration of the southern bend of the main channel, the latter increases in length over time. As a result, the MOW has less energy when arriving in its northernmost part, the flow having too little energy to maintain a connected, active secondary channel north of the main channel. As a consequence, the active

secondary channel (today's Gil Eanes) migrates progressively southwards. The second mechanism has tectonic causes. The southward migration of the channels would in this case be explained by a progressive regional tilting towards the south or southwest.

Conclusions

This paper brings new findings about the Gulf of Cadiz on the basis of a wealth of recent acoustic data.

The first point confirms the structural control of flow circulation in the gulf. Major channels have structural orientations and are bordered by linear rock escarpments and rounded structures interpreted as diapirs.

The second point concerns the morphodynamic evolution of the northern part of the Gulf of Cadiz. Besides being routed along the Gil Eanes channel, the MOW is also partly channelled through a northern, a central and a southern channel. The upper part of the deep core of the MOW spills over the southern channel embankment to form deposits characterized by sediment waves.

The third point is related to the overspreading of mass-wasting processes. High sedimentation rates associated with the continuous east–west shearing of the MOW flows induces intense sediment deformations, failures and mass flows. Frequent earthquakes with their epicentres located in the Gulf of Cadiz or in the neighbouring areas probably contribute to the triggering of slope failures and the formation of pockmarks. Fluid escape could also play a part in failure initiation.

The fourth point concerns the formation of minor channels. The slope failures evolve progressively towards the formation of secondary channels such as Gil Eanes channel. The active channel position tends to migrate south with time, which may result in autocyclic or allocyclic migration due to tectonic forcing.

The second and third points suggest that the Gulf of Cadiz is a complex, giant deep-sea contourite system with a hypertrophied left-hand side levee which shares strong similarities with channel-levee complexes built by particle-laden gravity processes. This comparison is emphasized by the presence of small terminal lobes developing at the mouth of secondary channels, probably due to loss of flow competence at the place where channels enlarge.

Acknowledgements We thank GENAVIR and the crew of the RV "Le Suroît" for technical assistance during the Cadisar cruise, D.J.W. Piper and an anonymous reviewer for constructive remarks on the manuscript, and the editors of *Geo-Marine Letters* for polishing of the English. UMR CNRS 5805 contribution number 1463.

References

- Ambar I (1983) A shallow core of Mediterranean water off western Portugal. *Deep Sea Res* 30(6A):677–680
- Ambar I, Howe R, Abdullah MI (1976) A physical and chemical description of the Mediterranean outflow in the Gulf of Cadiz. *Dtsch Hydro Z* 29:58–68
- Argus DF, Gordon RG, Demets C, Stein S (1989) Closure of the Africa–Eurasia–North America plate motion circuit and tectonics of the Gloria fault. *J Geophys Res* 94:5585–5602
- Auzende J-M, Olivet J-L, Pastouret L (1981) Implications structurales et paléogéographiques de la présence de Messinien à l'ouest de Gibraltar. *Mar Geol* 43:9–18
- Belderson RH, Johnson MA, Kenyon NH (1982) Bedforms. In: Stride AH (ed) *Offshore tidal sands; processes and deposits*, Chapman and Hall, London, pp 27–57
- Damuth J (1975) Echo character of the Western Equatorial Atlantic floor and its relationship to the dispersal and distribution of terrigenous sediments. *Mar Geol* 18:17–45
- Faugères J-C, Gonthier E, Stow DAV (1984) Contourite drift molded by deep Mediterranean outflow. *Geology* 12:296–300
- Faugères J-C, Cremer M, Monteiro H, Gaspar L (1985a) Essai de reconstitution des processus d'édification de la ride sédimentaire du Faro (marge sud-portugaise). *Bull Inst Géol Bassin Aquitaine* 37:229–258
- Faugères J-C, Frappa M, Gonthier E, Grousset FE (1985b) Impact de la veine d'eau méditerranéenne sur la sédimentation de la marge sud et ouest ibérique au Quaternaire récent. *Bull Inst Géol Bassin Aquitaine* 37:259–287
- Faugères J-C, Gonthier E, Mulder T, Kenyon NH, Cirac P, Griboulard R, Berné S, Le Suavé R (2002) Multi-process generated sediment waves on the Landes Plateau (Bay of Biscay, North Atlantic). *Mar Geol* 182:279–302
- Faugères J-C, Stow DAV, Imbert P, Viana A (1999) Seismic features diagnostic of contourite drifts. *Mar Geol* 12:1–38
- Gardner JV (2000) Mud diapirism and mud volcanism study. Introduction and geological setting. In: IOC Technical Series no 56, Part IV, Gulf of Cadiz/Moroccan margin, pp 56–57
- Gardner JV, Kidd RB (1983) Sedimentary processes on the Iberian continental margin viewed by long-range side-scan sonar. Part 1. Gulf of Cadiz. *Oceanol Acta* 6(3):245–253
- Gardner JV, Shashkin P (2000) Mud diapirism and mud volcanism study. Sidescan sonar data. In: IOC Technical Series no 56, Part IV, Gulf of Cadiz/Moroccan margin, pp 59–67
- Gervais A, Mulder T, Migeon S, Bonnel C, Cremer M (2000) Sedimentary record of deep contour currents in the Gulf of Cadiz: record of the Mediterranean outflow during the late Quaternary. 3rd Symposium, The Iberian Atlantic margin, 24–27 September 2000, Faro, Spain
- Gervais A, Mulder T, Savoye B, Migeon S. (2001) Recent processes of levee formation on the Zaire deep-sea fan. *C R Acad Sci Paris* 332:371–378
- Gonthier E, Faugères J-C, Stow DAV (1984) Contourite facies of the Faro drift, Gulf of Cadiz. In: Stow DAV, Piper DJW (eds) *Fine grained sediments: deep water processes and facies*. *Geol Soc, Spec Publ* no 4, pp 275–292
- Grousset FE, Joron J-L, Biscaye PE, Latouche C, Treuil M, Maillet N, Faugères J-C, Gonthier E (1988) Mediterranean outflow through the Strait of Gibraltar since 18,000 years B.P.: mineralogical and geochemical arguments. *Geo-Mar Lett* 8:25–34
- Griboulard R, Deniaud Y, Gonthier E (2001) Observation des déformations superficielles par submersible et imagerie sonar SAR d'un pli d'accrétion (prisme Sud-Barbade, océan Atlantique). *C R Acad Sci Paris* 330:281–287
- Gutscher M-A, Malod J, Réhault J-P, Contrucci I, Klingelhöfer F, Mendes-Victor L, Spakman W, SISMAR scientific team (2002) Evidence for active subduction beneath Gibraltar. *Geology* (in press)
- Heezen B, Johnson (1969) Mediterranean undercurrent and microphysiography west of Gibraltar. *Bull Inst Oceanogr Monaco* 67(1382):1–95
- Johnson J, Ambar I, Serra N, Stevens I (2002) Comparative studies of the spreading of Mediterranean water through the Gulf of Cadiz. *Deep Sea Res Part II: Topical Stud Oceanogr* 49(19):4179–4193

- Kenyon NH (1970) Sand ribbons of European tidal seas. *Mar Geol* 9:25–39
- Kenyon NH, Belderson RH (1973) Bed-forms of the Mediterranean undercurrent observed with side-scan sonar. *Sediment Geol* 9:77–99
- Kenyon NH, Akhmetzhanov A, Ivanov M (2000) Multidisciplinary study of geological processes on the North East Atlantic and western Mediterranean margins. Preliminary results of geological and geophysical investigations during the TTR-9 cruise of R/V “Professor Logachev”, June–July 1999. Intergovernmental Oceanographic Commission Technical Series 56
- Lajat D Biju-Duval B, Gonnard R, Letouzey J, Winnock E (1975) Prolongement dans l’Atlantique de la partie externe de l’arc bético-rifain. *Bull Soc Géol Fr* 7(4):481–485
- Lewis KB (1971) Slumping on a continental slope inclined at 1°–4°. *Sedimentology* 16:97–110
- Madelain F (1970) Influence de la topographie du fond sur l’écoulement méditerranéen entre le détroit de Gibraltar et le Cap Saint Vincent. *Cahiers Océanogr* 22:43–61
- Maldonado A, Somoza L, Pallarés L (1999) The Betic orogen and the Iberian–African boundary in the Gulf of Cadiz: geological evolution (central North Atlantic). *Mar Geol* 155:9–43
- Malod JA (1982) Comparaison de l’évolution des marges continentales au Nord et au Sud de la péninsule Ibérique. Thèse Doctorat d’Etat, Université Paris 6, no 82.23
- McCave IN, Tucholke BE (1986) Deep current-controlled sedimentation in the western North Atlantic. In: Vogt PR, Tucholke BE (eds) *The geology of North America, vol M. The western North Atlantic region, decade of North America Geology*. Geological Society of America, Boulder, CO, pp 451–468
- Meincke J, Siedler G, Zenk W (1975) Some current observations near the continental slope off Portugal. *Meteor Forsch Ergeb* A(16):15–22
- Melières F (1974) Recherches sur la dynamique sédimentaire du Golfe de Cadix (Espagne). Thèse Doctorat d’Etat, Université Paris 6, no A10206
- Migeon S (2000) Dunes géantes et levées sédimentaires en domaine marin profond: approche morphologique, sismique et sédimentologique. Thèse Université Bordeaux 1
- Migeon S, Savoye B, Faugères J-C (2000) Quaternary development of migrating sediment waves in the Var deep-sea fan: distribution, growth pattern and implication for levee evolution. *Sediment Geol* 113:265–293
- Migeon S, Savoye B, Zanella E, Mulder T, Faugères J-C, Weber O (2001) Detailed seismic-reflection and sedimentary study of turbidite sediment waves on the Var Sedimentary Ridge (SE France): significance for sediment transport and deposition and for the mechanism of sediment-wave construction. *Mar Petrol Geol* 18:179–208
- Mougenot D (1988) Géologie de la marge portugaise. Thèse Doctorat d’Etat, Université Paris 6
- Mougenot D, Vanney JR (1982) Les rides de contourites Plio-Quaternaires de la pente continentale sud-portugaise. *Bull Inst Géol Bassin Aquitaine* 31:131–139
- Nelson CH, Baraza J, Maldonado A (1993) Mediterranean undercurrent sandy contourites, Gulf of Cadiz, Spain. In: Stow DAV, Faugères J-C (eds) *Contourites and bottom currents. Contourites and hemipelagites in the deep-sea*. *Sediment Geol* 82:103–131
- Nelson CH, Baraza J, Maldonado A, Rodero J, Escutia C, Barber JH Jr (1999) Influence of the Atlantic inflow and Mediterranean outflow currents on Quaternary sedimentary facies of the Gulf of Cadiz continental margin. In: Maldonado A, Nelson CH (eds) *Evolution of the Iberian Margin and the Gulf of Cadiz*. *Mar Geol* 155:99–129
- Normark WR (1970) Growth patterns of deep sea fans. *AAPG Bull* 54:2170–2195
- Peakall JD, McCaffrey WD, Kneller BC, Stelling CE, McHargue TR, Schweller WJ (2000) A process model for the evolution of submarine fan channels: implications for sedimentary architecture. In: Bouma AH, Stone CG (eds) *Fine-grained turbidite system*. AAPG Memoir, 72/SEPM Spec Publ 68, pp 73–88
- Piper DJW, Normark WR (1983) Turbidite depositional patterns and flow characteristics, navy submarine fan, California Borderland. *Sedimentology* 30:681–694
- Prior DB, Coleman JM (1979) Submarine landslides geometry and nomenclature. *Z Geomorphol* 23:415–426
- Schönfeld J, Zahn R (2000) Late glacial to Holocene history of the Mediterranean outflow. Evidence from benthic foraminiferal assemblages and stable isotopes at the Portuguese margin. *Palaeogeogr Palaeoclimatol Palaeoecol* 159:85–111
- Somoza L, Hernandez-Molina FJ, De Andres JR, Rey J (1997) Continental shelf architecture and sea-level cycles: late Quaternary high-resolution stratigraphy of the Gulf of Cadiz, Spain. *Geo-Mar Lett* 17:133–139
- Srisvastava SP, Schouten H, Roest WR, Klitgord KD, Kovacs LC, Verhoef J, Macnab R (1990) Iberian plate kinematics: a jumping plate boundary between Eurasia and Africa. *Nature* 344:756–759
- Stow DAV, Faugères J-C, Gonthier E (1986) Facies distribution and drift growth during the late Quaternary (Gulf of Cadiz). *Mar Geol* 72:71–100
- Thorpe SA (1972) A sediment cloud below the Mediterranean outflow. *Nature* 236:326–327
- Thorpe SA (1976) Variability of the Mediterranean undercurrent in the Gulf of Cadiz. *Deep-Sea Res* 23:711–727
- Vergnaud-Grazzini C, Caralp M, Faugères J-C, Gonthier E, Grousset FE, Pujol C, Salièges J-F (1989) Mediterranean outflow through the Strait of Gibraltar since 18 ky B.P. *Oceanol Acta* 12(4):305–324
- Viana A (1998) Le rôle et l’enregistrement des courants océaniques dans les dépôts de marges continentales: la marge du bassin sud-est brésilien. Thèse Université Bordeaux 1
- Viana A, Faugères J-C, Stow DAV (1998) Bottom-current-controlled sand deposits—a review of modern shallow to deep-water environments. *Sediment Geol* 115:53–80
- Zahn R, Sarnthein M, Erlenkeuser H (1987) Benthic isotope evidence for changes of the Mediterranean outflow during the Late Quaternary. *Paleoceanography* 2(6):543–559
- Zitellini N, Chierici F, Sartori R, Torelli L (1999) The tectonic source of the 1755 Lisbon earthquake and tsunami. *Ann Geofis* 42:49–55